

Oscillon dominance and symmetric excitations of the Abelian-Higgs “classical vacuum”

F.K. Diakonov^a G.C. Katsimiga^a X.N. Maintas^a C.E. Tsagkarakis^a

^a*Department of Physics, University of Athens
GR-15784 Athens, Greece*

ABSTRACT: We study the formation of oscillons in the classical Abelian-Higgs model in the case of strongly broken gauge symmetry. In this limit the wells of the potential of the scalar field are sufficiently deep, presenting a scenario far from the associated critical point. Using a multiscale perturbation expansion, the equations of motion for the fields are reduced to a system of coupled nonlinear Schrödinger equations (CNLS). Exact solutions of the latter are used to obtain approximate analytical solutions for both the gauge and Higgs field in the form of oscillons and oscillating kinks. We explore the persistence of these solutions for a wide range of the model’s single parameter which is the ratio of the Higgs to the gauge field mass. We show that only oscillons which describe a Higgs field oscillating symmetrically with respect to its “classical vacuum”, are long lived. Furthermore plane waves and oscillating kinks are shown to decay into oscillon-like patterns, due to the modulation instability mechanism. This suggests that oscillons dominate the solution space of the model. Numerical simulations of the exact dynamics verify both, the robustness of the analytically obtained oscillon solutions as well as the decay of plane waves and oscillating kinks.

Contents

1	Introduction	1
2	General formalism and setup	3
2.1	Deriving the NLS equations	3
2.2	Soliton solutions of the NLS equations and approximate oscillons and oscillating kinks	5
2.3	Modulation Instability	7
3	Numerical results: oscillon’s longevity	9
4	Conclusions and discussion	12

1 Introduction

The study of oscillons in nonlinear field theories, introduced in the seminal works of Refs. [1, 2], still continues to attract considerable attention. This is mainly due to the fact that such field configurations appear abundantly in systems involving spontaneously broken symmetries, and they are long-lived. Although oscillons are known to radiate, they possess—depending on the dimensionality of the embedding space—extremely large lifetimes, as estimated from analytical calculations and numerical simulations [3–5].

For scalar field theories in $(1 + 1)$ space-time dimensions [4, 6] oscillons once formed, (e.g. via kink-antikink collisions or by using *sech*-shaped initial conditions) are found to be persistent, decaying eventually through radiation [3]. Estimations of the decay rate of oscillons were made not only at the classical [4] but also in the quantum level [5]. In two space dimensions (2-D) numerical simulations confirm the existence and longevity of oscillons, starting from a gaussian ansatz [7–9]. Oscillons can also be formed in three dimensional (3-D) spherically symmetric scalar field theories with gaussian initial conditions [13], particularly in the context of bubble dynamics [10–12]. In (3-D) the critical parameters for oscillon formation are the initial amplitude and energy (see also Ref. [14]), while even in this case once an oscillon is formed, is found to be extremely long lived.

Oscillons were also studied both numerically and analytically in scalar ϕ^4 models with generalized potentials in $(D + 1)$ space-time dimensions [15–17], as well as in models including gauge fields, either in Abelian or non-Abelian gauge theories. In particular they were found in the Abelian Higgs model as debris of sphaleron decay [18], or as small amplitude approximate solutions of a Nonlinear Schrödinger equation (NLS) [19] in $(1 + 1)$ -dim, as remnants of vortex-antivortex annihilation [20] in $(2 + 1)$ -dim, and from flux-antiflux tube annihilation [21] in $(3 + 1)$ -dim. Numerical simulations [22] and analytical investigations [23] in the context of non-Abelian [SU(2)] Higgs theory in (3-D) also verified the

existence of oscillons. Finally, oscillons were also found in the $SU(2) \times U(1)$ model without fermions [24].

Oscillon formation is employed in cosmology to study the dynamics of the early universe. In particular it was shown in Refs. [25–32], that oscillons, formed during reheating in the post inflation epoch or during non-thermal symmetry breaking phase transitions driven by rapid fluctuations, may contribute a significant fraction of the total energy density of the universe. Efforts were also made, to link oscillons with the phenomenology of superconductivity [21] in the context of the Abelian-Higgs model, using the ratio m_H/m_A (where m_H is the mass of the Higgs field and m_A the mass of the gauge field) to distinguish type-I from type-II superconductors.

In most of the above mentioned studies, oscillons were obtained numerically. Approximate analytical solutions describing oscillons were rigorously derived in [19] by introducing multiple scale perturbation expansion [33] in gauge theories [34], and assuming a sufficiently small amplitude for the Higgs field. In this limit it was found that the scalar field performs asymmetric oscillations around the “classical vacuum”. Such a scenario occurs naturally considering the model just after the symmetry breaking i.e. close to the critical point. Then the minimum of the scalar field potential is very flat and the dominating quartic terms lead to an asymmetric shape of the potential around it.

In the present work we investigate the Abelian-Higgs model in a different limit, where the gauge and the scalar field amplitudes are of the same order. This scenario corresponds to a strong breaking of the underlying gauge symmetry, far beyond the related critical point. In this case the minimum of the potential occurs at the bottom of a deep well, while the potential shape is almost symmetric around it. Employing this assumption for the field amplitudes, within the framework of multiple scale perturbation theory [34] we derive a system of CNLS equations describing the field envelopes. Using the results presented in Ref. [35], we solve analytically the coupled system obtaining bright-bright, dark-bright and dark-dark soliton solutions. Our analysis shows that only bright-bright solitons may describe long-lived oscillons of the original equations of motion, with both fields performing symmetric oscillations around the “classical vacuum”. Additionally, it is shown that any dark component is subject to the modulation instability (MI) mechanism [36]. Subsequently, we integrate numerically the exact equations of motion and we verify that the analytically obtained solutions describe the long-lived oscillons sufficiently well. Surprisingly enough, even when the perturbation expansion is not valid, using initial conditions corresponding to bright-bright solitons, we numerically obtain long-lived oscillons. Furthermore, we use the MI mechanism in order to illustrate that oscillons may be formed for all values of the parameter m_H/m_A . This leads us to the conclusion that oscillons dominate in the solution space of the Abelian-Higgs model.

The paper is organized as follows: in section II, we present the equations of motion for the Abelian-Higgs model reducing them to a CNLS system with the method of multiple scales and provide the corresponding analytical solutions. In section III we present results of direct numerical integration of the original equations of motion to check the validity of our approximations and study the stability of the analytically found solutions. Finally, in section IV we present our concluding remarks.

2 General formalism and setup

2.1 Deriving the NLS equations

The Lagrangian density of the model has the form:

$$\mathcal{L} = -\frac{1}{4}F_{\mu\nu}F^{\mu\nu} + (D_\mu\Phi)^*(D^\mu\Phi) - V(\Phi^*\Phi), \quad (2.1)$$

where Φ is a complex scalar field, $D_\mu = \partial_\mu + ieA_\mu$ is the covariant derivative with e the coupling constant, and $F_{\mu\nu}$ is the electromagnetic tensor. The potential $V(\Phi^*\Phi)$ has the form:

$$V(\Phi^*\Phi) = \mu^2\Phi^*\Phi + \lambda(\Phi^*\Phi)^2, \quad (2.2)$$

with $\mu^2 < 0$ and $\lambda > 0$ being undefined constants. For the spontaneously broken symmetry case, we choose as vacuum the minimum $v = \sqrt{-\mu^2/2\lambda}$ of the potential given by Eq. (2.2). We expand the Φ field around this vacuum expectation value (vev) as $\Phi = v + H/\sqrt{2}$, gauging away the Goldstone mode. H is a real scalar field, the Higgs field, with mass $m_H = \sqrt{2\lambda}v$. Due to the symmetry breaking the gauge field A_μ acquires mass $m_A = ev$.

We consider the ansatz: $A_0 = A_1 = A_3 = 0$ and $A_2 = A(x, t)$ which is compatible with the Lorentz condition in (1 + 1)-dim and simplifies significantly the equations of motion. Defining dimensionless variables: $\tilde{x}^\mu = m_A x^\mu$, $\tilde{A} = (e/m_A)A$, $\tilde{H} = (e/m_A)H$ [vev is also scaled as $\tilde{v} = (e/m_A)v$], and dropping the tildes after this substitution, the corresponding equations of motion become:

$$(\square + 1)A + 2HA + H^2A = 0, \quad (2.3)$$

$$(\square + q^2)H + \frac{3}{2}q^2H^2 + \frac{q^2}{2}H^3 + A^2(1 + H) = 0, \quad (2.4)$$

where $H = H(x, t)$, while $q \equiv m_H/m_A$ is the single dimensionless parameter that designates the dynamics. We are interested in finding localized solutions to the above system of equations i.e. Eqs. (2.3)-(2.4). For this purpose we employ multiple scale perturbation theory [33] expanding space-time coordinates and their derivatives as follows: $x_0 = x$, $x_1 = \epsilon x$, $x_2 = \epsilon^2 x, \dots$, $t_0 = t$, $t_1 = \epsilon t$, $t_2 = \epsilon^2 t, \dots$, $\partial_x = \partial_{x_0} + \epsilon\partial_{x_1} + \dots$, $\partial_t = \partial_{t_0} + \epsilon\partial_{t_1} + \dots$. Accordingly we write the gauge and the scalar field as:

$$A = \epsilon A^{(1)} + \epsilon^2 A^{(2)} + \dots, \quad (2.5)$$

$$H = \epsilon H^{(1)} + \epsilon^2 H^{(2)} + \dots, \quad (2.6)$$

where ϵ is a formal small parameter: $0 < \epsilon \ll 1$, related to the amplitude of the Higgs and the gauge field excitations around the physical vacuum. Inserting Eqs. (2.5)-(2.6) into Eqs. (2.3)-(2.4), and expressing the operators in terms of the slow scales mentioned above, we proceed in our analysis solving the equations of motion order by order. To first order in ϵ we have the following decoupled equations for the gauge (A) and the Higgs (H) field respectively:

$$\mathcal{O}(\epsilon): (\square_0 + 1) A^{(1)} = 0, \quad (2.7)$$

$$(\square_0 + q^2) H^{(1)} = 0. \quad (2.8)$$

Equations (2.7) and (2.8), acquire plane wave solutions of the form:

$$A^{(1)} = f e^{i\theta_1} + f^* e^{-i\theta_1}, \quad (2.9)$$

$$H^{(1)} = l e^{i\theta_2} + l^* e^{-i\theta_2}, \quad (2.10)$$

where “*” denotes complex conjugate, while $f = f(x_i, t_i)$ and $l = l(x_i, t_i)$ are functions of the slow variables that have to be determined (the index $i = 1, 2, \dots$ refers to the slow scales). The phase θ_j is defined as: $\theta_j \equiv k_j x - \omega_j t$, where the index $j = 1, 2$ refers to the gauge and the scalar field respectively. Substituting Eqs. (2.9) and (2.10) into Eqs. (2.7)-(2.8) we get the dispersion relations for the two fields i.e. $\omega_1^2 = k_1^2 + 1$ and $\omega_2^2 = k_2^2 + q^2$. Thus, to first order in ϵ the linear limit of the theory is recovered. Proceeding to the next order of the perturbation scheme, namely $\mathcal{O}(\epsilon^2)$, we obtain the following system of equations:

$$(\square_0 + 1) A^{(2)} = -2\partial_{\mu_0} \partial^{\mu_1} A^{(1)} - 2H^{(1)} A^{(1)}, \quad (2.11)$$

$$(\square_0 + q^2) H^{(2)} = -2\partial_{\mu_0} \partial^{\mu_1} H^{(1)} - \left(\frac{3q^2}{2} H^{(1)2} + A^{(1)2} \right), \quad (2.12)$$

Notice that the first terms on the right hand side of the above equations, are “*secular*”, that is in resonance with the operators on the left side. These terms imply a linear growing of $A^{(2)}$, $H^{(2)}$ with time and therefore lead to the blow-up of the solutions. Consequently, in order for the perturbation scheme to be valid, these terms have to vanish independently, leading to the following equations for $f = f(x_i, t_i)$ and $l = l(x_i, t_i)$:

$$\hat{L}_1 f = 0, \quad (2.13)$$

$$\hat{L}_2 l = 0. \quad (2.14)$$

The operator \hat{L}_j is defined as $\hat{L}_j \equiv -i \left(\partial_{t_1} + v_g^{(j)} \partial_{x_1} \right)$, with $v_g^{(j)} \equiv \partial \omega_j(k) / \partial k_j = k_j / \omega_j$ being the group velocities for the gauge ($j=1$) and the Higgs ($j=2$) field respectively. Eqs. (2.13)-(2.14) are automatically satisfied if $f = f(X_1, t_2)$ and $l = l(X_2, t_2)$ where $X_j \equiv x_1 - v_g^{(j)} t_1$.

Furthermore, Eqs. (2.11)-(2.12) can be solved analytically and the solutions for the fields $A^{(2)}$ and $H^{(2)}$ as functions of f and l have the following form:

$$A^{(2)} = \frac{fl}{a} e^{i\Theta_+} + \frac{fl^*}{b} e^{i\Theta_-} + c.c., \quad (2.15)$$

$$H^{(2)} = \frac{l^2}{2} e^{2i\theta_2} + \frac{f^2}{4 - q^2} e^{2i\theta_1} - \frac{3q^2 |l|^2 + 2|f|^2}{q^2} + c.c., \quad (2.16)$$

where “c.c.”, stands for the complex conjugate, while $a = \omega_1 \omega_2 - k_1 k_2 + q^2/2$, $b = k_1 k_2 - \omega_1 \omega_2 + q^2/2$ and $\Theta_{\pm} \equiv \theta_1 \pm \theta_2$. Note, that the coefficients in equations (2.15)-(2.16), e.g. $1/b$, define regions for the parameter q for which the fields $A^{(2)}$ and $H^{(2)}$ could become infinitely large, [in the perturbation are assumed to be of $\mathcal{O}(1)$]. Such regions are for consistency excluded in our analysis. Also notice that once the functions f and l are determined, the solutions for $A^{(2)}$ and $H^{(2)}$ are also fixed. Continuing our analysis we get in $\mathcal{O}(\epsilon^3)$ the

following equations:

$$\begin{aligned} (\square_0 + 1) A^{(3)} &= -2\partial_{\mu_0} \partial^{\mu_1} A^{(2)} - (\square_1 + 2\partial_{\mu_0} \partial^{\mu_2}) A^{(1)} \\ &\quad - 2 \left(H^{(2)} A^{(1)} + A^{(2)} H^{(1)} \right) - H^{(1)2} A^{(1)}, \end{aligned} \quad (2.17)$$

$$\begin{aligned} (\square_0 + q^2) H^{(3)} &= -2\partial_{\mu_0} \partial^{\mu_1} H^{(2)} - (\square_1 + 2\partial_{\mu_0} \partial^{\mu_2}) H^{(1)} \\ &\quad - 3q^2 H^{(1)} H^{(2)} - \frac{q^2}{2} H^{(1)3} - 2A^{(1)} A^{(2)} - A^{(1)2} H^{(1)}. \end{aligned} \quad (2.18)$$

The first terms on the right hand side of Eqs. (2.17)-(2.18) can be eliminated through the aforementioned choice for the variables X_i along with the condition $v_g^{(1)} = v_g^{(2)}$. Furthermore, to simplify the calculations remaining consistent, we choose $k_1 = k_2 = 0$, i.e. $v_g^{(1)} = v_g^{(2)} = 0$ so that $X_1 = X_2 = x_1$. Additionally, at the same order, the solvability condition requires the *secular* parts of Eqs. (2.17)-(2.18) to vanish, leading to the following equations: $(\square_1 + 2\partial_{\mu_0} \partial^{\mu_2} + 2H^{(2)} + H^{(1)2}) A^{(1)} + 2A^{(2)} H^{(1)} = 0$, and $(\square_1 + 2\partial_{\mu_0} \partial^{\mu_2} + 3q^2 H^{(2)} + q^2/2 H^{(1)2} + A^{(1)2}) H^{(1)} + 2A^{(1)} A^{(2)} = 0$. With the above assumptions we derive a system of CNLS equations for the functions $f(x_1, t_2)$ and $l(x_1, t_2)$:

$$i\partial_{t_2} f = -\frac{1}{2}\partial_{x_1}^2 f + g_{11}|f|^2 f + g_{12}|l|^2 f, \quad (2.19)$$

$$iq\partial_{t_2} l = -\frac{1}{2}\partial_{x_1}^2 l + g_{21}|f|^2 l + g_{22}|l|^2 l, \quad (2.20)$$

where $g_{ij} \equiv g_{ij}(q)$ are the following functions of q :

$$\begin{aligned} g_{11} &= -\left(\frac{2}{q^2} + \frac{1}{q^2 - 4}\right), \quad g_{12} = -\left(2 - \frac{4}{q^2 - 4}\right) \\ g_{21} &= g_{12}, \quad g_{22} = -3q^2. \end{aligned} \quad (2.21)$$

2.2 Soliton solutions of the NLS equations and approximate oscillons and oscillating kinks

The system of Eqs. (2.19)-(2.20), in the limit $g_{ij} = 1$, is reduced to the integrable Manakov model [37], which admits exact analytical solutions. For $g_{ij} \neq 1$ analytical soliton solutions of the CNLS system can also be obtained, as it was shown in a recent work [35]. In our case the coupling constants g_{ij} depend on the parameter q (cf. Fig. 1) and in general $g_{ij} \neq 1$. Adopting the method of [35] we show below that solitons can be obtained in different q regions. First we look for solutions in the form of bright-bright (*bb*) solitons using the following ansatz:

$$f_{bb} = a_1 \operatorname{sech}(\beta_{bb} x_1) e^{-i\nu_1 t_2}, \quad (2.22)$$

$$l_{bb} = a_2 \operatorname{sech}(\beta_{bb} x_1) e^{-i\nu_2 t_2}, \quad (2.23)$$

where $a_{1,2}$ denote the amplitudes, $\nu_{1,2}$ the frequencies of the solitons, and β_{bb} is the inverse width of the solitons. The condition that the squared amplitudes and widths of the solutions are positive defines three regions of the single parameter q where *bb* solitons can be found,

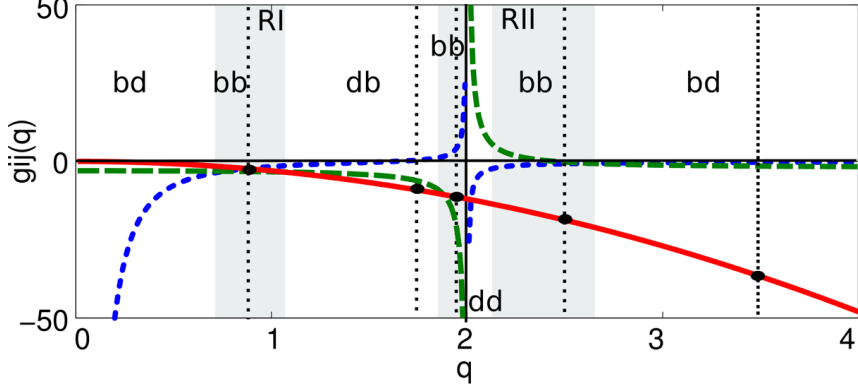


Figure 1: (Color online): Sketch showing the regions of existence of each type of solution, depending on different values of the parameter q . Dotted [blue] lines correspond to $g_{11}(q)$, solid [red] line to $g_{22}(q)$, and dashed [green] lines to $g_{12}(q) = g_{21}(q)$. Moreover dashed [black] lines at $q = 0.88$, $q = 1.75$, $q = 1.95$, $q = 2.5$ and $q = 3.5$ respectively, correspond to the parameters used for the simulations given below.

i.e. $0.76 < q < 1.06$, $1.88 < q < 2$ and $2.13 < q < 2.63$. Another type of solution, in the form of dark-dark (dd) solitons, can also be obtained using the ansatz

$$f_{dd} = a_1 \tanh(\beta_{dd}x_1) e^{-i\nu_1 t_2}, \quad (2.24)$$

$$l_{dd} = a_2 \tanh(\beta_{dd}x_1) e^{-i\nu_2 t_2}. \quad (2.25)$$

The aforementioned condition for the amplitudes and widths implies that solutions of this type are allowed in the region $2 < q < 2.13$. Finally, bright-dark (bd) vector soliton solutions (f, l) of the form:

$$f_{bd} = a_1 \operatorname{sech}(\beta_{bd}x_1) e^{-i\nu_1 t_2}, \quad (2.26)$$

$$l_{bd} = a_2 \tanh(\beta_{bd}x_1) e^{-i\nu_2 t_2}, \quad (2.27)$$

as well as dark-bright (db) solutions (by interchanging $f_{bd} \leftrightarrow l_{bd}$) can also be found. Solitons of the bd (db) type are possible in the regions $0 < q < 0.76$, $q > 2.63$ ($1.06 < q < 1.88$). In all cases the soliton widths, amplitudes and frequencies are connected through the equations shown in Table 1. Figure 1 shows the coupling constants g_{ij} as functions of q , and the region of existence for each different vector soliton is highlighted. Using Eqs. (2.9)-(2.10) and the aforementioned soliton solutions of Eqs. (2.19)-(2.20) we can obtain localized approximate solutions (to order ϵ) for the fields A and H :

$$A(x, t) \approx 2\epsilon |f(\epsilon\beta x)| \cos(1 + \epsilon^2\nu_1) t, \quad (2.28)$$

$$H(x, t) \approx 2\epsilon |l(\epsilon\beta x)| \cos(q + \epsilon^2\nu_2) t. \quad (2.29)$$

Inserting the profiles of f, l in Eqs. (2.28)-(2.29), we obtain different classes of approximate solutions. Those corresponding to bb -solitons as in Eqs.(2.22)-(2.23), will have the form of oscillons for both fields. On the other hand dd -solitons correspond to solutions where both fields have the form of oscillating kinks. Finally bd (db) solitons will result in an oscillon for the field A (H) and an oscillating kink for H (A).

Table 1: Normalized amplitudes-widths and frequencies

Regions	$(a_2/a_1)^2$	$(\beta/a_1)^2$	(ν_1/ν_2)
bb	$(g_{11} - g_{21}) / (g_{22} - g_{12})$	$(g_{12}g_{21} - g_{11}g_{22}) / (g_{22} - g_{11})$	q
dd	$(g_{11} - g_{21}) / (g_{22} - g_{12})$	$(g_{11}g_{22} - g_{12}g_{21}) / (g_{22} - g_{12})$	q
db	$(g_{11} - g_{21}) / (g_{12} - g_{22})$	$(g_{12}g_{21} - g_{11}g_{22}) / (g_{12} - g_{22})$	$\frac{2qg_{11}(g_{12} - g_{22})}{(g_{21}g_{12} - 2g_{12}g_{22} + g_{11}g_{22})}$
bd	$(g_{11} - g_{21}) / (g_{12} - g_{22})$	$(g_{11}g_{22} - g_{12}g_{21}) / (g_{12} - g_{22})$	$\frac{-2qg_{11}(g_{12} - g_{22})}{(g_{21}g_{12} - 2g_{12}g_{22} + g_{11}g_{22})}$

2.3 Modulation Instability

In this section we will explore the impact of the modulation instability mechanism to the solution space of the Abelian-Higgs model. To this end, we examine the stability of plane wave solutions of the CNLS Eqs. (2.19)-(2.20). The mechanism of modulation instability (MI) [36] is an important property of the NLS equation, revealing localized structures that a system supports, e.g. *sech* – *shaped* solutions of the form of Eqs. (2.22)-(2.23). This mechanism also gives information about the *tanh* – *shaped* solutions, e.g. Eqs. (2.24)-(2.25), since instability of plane waves leads to unstable background for this type of solutions. We consider the following ansatz:

$$f(x_1, t_2) = (f_0 + \delta f) e^{-i\Omega_1 t_2}, \quad (2.30)$$

$$l(x_1, t_2) = (l_0 + \delta l) e^{-i\Omega_2 t_2}, \quad (2.31)$$

where f_0 and l_0 are the amplitudes of the plane wave solutions of the CNLS equations, and $\Omega_{1,2}$ are their frequencies satisfying the dispersion relations

$$\omega_1 \Omega_1 = g_{11}|f_0|^2 + g_{12}|l_0|^2, \quad (2.32)$$

$$\omega_2 \Omega_2 = g_{21}|f_0|^2 + g_{22}|l_0|^2. \quad (2.33)$$

The small amplitude perturbations i.e. $\delta f/f, \delta l/l \ll 1$, are complex functions of the form $\delta f = u_1 + iw_1$, $\delta l = u_2 + iw_2$. The real functions u_j, w_j are considered to be of the general form:

$$u_j = u_{0j} \exp[i(Kx_1 - \Omega t_2)] + c.c., \quad (2.34)$$

$$w_j = w_{0j} \exp[i(Kx_1 - \Omega t_2)] + c.c., \quad (2.35)$$

where the amplitudes u_{0j}, w_{0j} are constants while K is the wavenumber and Ω the frequency of the perturbation. Substituting Eqs. (2.34)-(2.35) to the CNLS Eqs. (2.19)-(2.20) leads to an algebraic system of equations, the determinant of which has to be zero. This compatibility condition leads to the following equation:

$$A\Omega^4 - (\omega_1^2 B_2 + \omega_2^2 B_1) \Omega^2 + (B_1 B_2 - \Gamma) = 0, \quad (2.36)$$

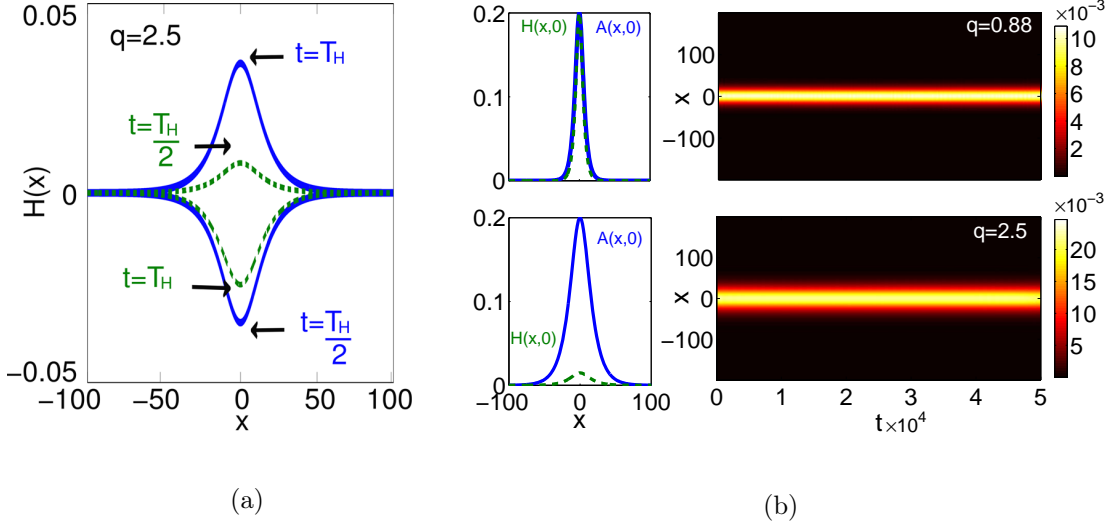


Figure 2: (Color online): Panel (a) shows a plot of the Higgs field for $t = T_H$, $t = T_H/2$ and $q = 2.5$. Solid (blue) lines refer to the symmetric oscillations of the field $H(x)$. For comparison, in the same figure dashed (green) lines depict the oscillon in the asymmetric case.

Panel (b): left panels depict the profiles of the two fields A [solid (blue) lines], and H [dashed (green) lines], for $t = 0$, corresponding to oscillon solutions of Eqs. (2.28)-(2.29) for different values of q . Right panels: contour plots showing the evolution of the energy density $E(x, t)$ for initial conditions corresponding to the left panel. The total time of integration is $t = 5 \times 10^4$ and the different values of q are depicted in the upper right corner of each contour.

where $A = (\omega_1 \omega_2)^2$, $B_j = K^2/2 (K^2/2 + 2g_{jj} f_0^2)$ with $j = 1, 2$ and $\Gamma = K^4 g_{12} g_{21} (f_0 l_0)^2$. Requiring real roots of Eq. (2.36) we are led to the following stability conditions:

$$g_{11} g_{22} - g_{12} g_{21} > 0, \quad g_{11} \geq 0, \quad g_{22} \geq 0. \quad (2.37)$$

As seen from Eq. (2.21), there are no real values of the parameter q satisfying the last inequality of Eq. (2.37). Thus plane wave solutions are unstable under small perturbations. The aforementioned result implies that solutions including d components, although they are allowed by the CNLS system in Eqs. (2.19)-(2.20), are expected to be unstable due to the modulation instability. This can be seen from the following fact: the dark-component in the solitons of Eqs. (2.24)-(2.27), takes asymptotically the form $\sim \pm a_i \exp[-i\nu_i t]$ at $x \rightarrow \pm\infty$. Hence away from its core, the solution is a plane wave and any perturbation will lead to the appearance of MI and the generation of oscillons. Thus we argue that localized solutions in the form of kinks, are not supported in the setting where A and H are of the same order.

According to the above analysis, the relevant solutions for the functions $f(x_1, t_2)$ and $l(x_1, t_2)$ are the bb solitons, which are found in the three regions defined in the previous paragraph by Eqs. (2.22)-(2.23) (see also shaded areas of Fig. 1). The profile of a Higgs field oscillon with $q = 2.5$, is shown in Fig. 2 (a) with a solid (blue) line, for a half and

total period of oscillation. Notice that in contrast to previous findings [19], the Higgs field performs symmetric oscillations around the “classical vacuum”(i.e $H = 0$). For comparison a typical solution of an asymmetric oscillon of Ref. [19] is shown [dashed (green) line] for the same value of q . As already discussed, the two types of oscillons (asymmetric, symmetric) describe different scenarios for the underlying physics: the asymmetric solutions are valid in the case of weakly broken symmetry, i.e. just beyond the associated critical point, while the symmetric solutions occur when the gauge symmetry is strongly broken, i.e. far beyond the critical point.

It is also important to note that in the region $1.88 < q < 2$, the amplitudes of the second order expansions of the fields [cf. Eqs. (2.15)-(2.16)] become larger than $\mathcal{O}(1)$ and the perturbation scheme collapses. Thus, in this case oscillon solutions are not expected to exist for the exact system. However, our numerical results show that an initial condition corresponding to bb solitons in this region also leads to robust oscillon solutions.

3 Numerical results: oscillon’s longevity

According to the analysis of the two previous sections, robust localized solutions of the original system of equations (2.3)-(2.4) in the form of NLS bright-bright solitons, are expected to be found in the two parameter regions $0.76 < q < 1.06$ (Region I) and $2.13 < q < 2.63$ (Region II) [cf. Fig. 1]. To clarify this issue we perform numerical integration of the exact system Eqs. (2.3)-(2.4) for a wide range of q values, using as initial conditions the approximate solutions Eqs. (2.28)-(2.29) for the case of bb -solitons. Our main interest is to confirm the existence of these structures and explore their long time dynamics. We use a fourth-order Runge-Kutta integrator for the time propagation with a lattice of length $L = 400$, lattice spacing $dx = 0.1$, time step $dt = 10^{-2}$ and $\epsilon = 0.1$. With this choice of parameters the numerical integration conserves the energy for the total time interval of our simulations up to the order of 10^{-3} .

In the top panel of Fig. 2 (b) we show an example of the evolution of an oscillon in Region I for $q = 0.88$. The top left panel depicts the oscillon profile at $t = 0$, where solid (blue) and dashed (green) lines present A and H respectively. The evolution of the energy density is shown in the top right panel for a time interval of $t = 5 \times 10^4$, corresponding to $\sim 10^4$ oscillations for both fields. The energy density remains localized throughout the simulation, indicating the robustness of the oscillons in Region I. We have confirmed (results not shown here) the existence and longevity of oscillons in Region I for different values of q .

Next, an example of an oscillon in Region II and for $q = 2.5$ is shown in the bottom panels of Fig. 2 (b). The evolution of the energy density in the right panel again confirms the existence of the respective oscillon solution and illustrates its longevity, since it turns out to be robust after performing at least $\sim 10^4$ oscillations. Note that for this example and for $q \in [2.3, 2.63]$ (Region II), the amplitude of H gets suppressed so that the ratio of the amplitudes of the fields H/A is close to the value of the perturbation parameter ϵ . In this sense for this region of parameter values one recovers the scenario of small Higgs amplitude, explored in our previous work [19]. However the solutions presented here have a

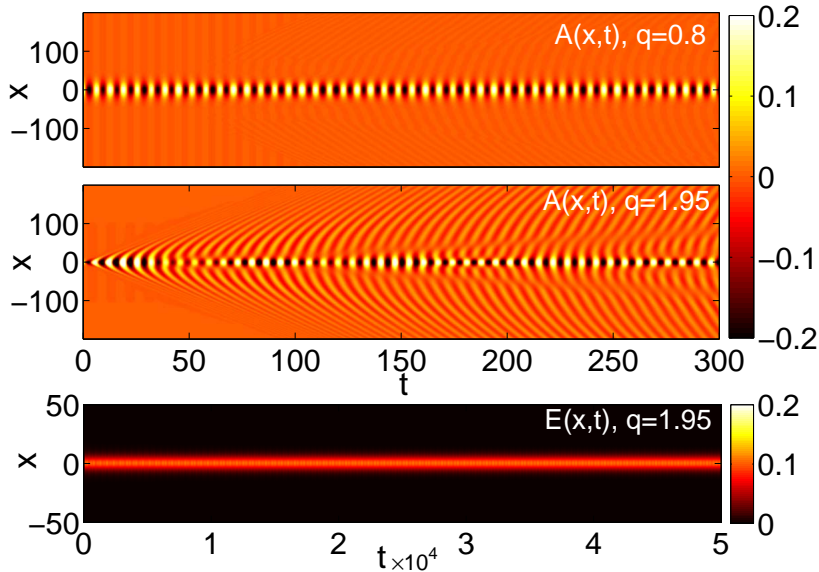


Figure 3: (Color online): Top and middle panels: Contour plots showing the evolution of the gauge field $A(x,t)$ for different values of q , as indicated in the upper right corner of each. Bottom: Contour of the energy density $E(x,t)$ for a time interval $t = 5 \times 10^4$.

different profile than those in [19]. In particular, the Higgs field in [19] exhibits asymmetric oscillations with respect to the origin (i.e. $H = 0$), while the oscillon of Eq. (2.29) is symmetric [see also Fig. 2 (a)]. Formally, this is due to the fact that the Higgs field in [19] obeys a linear equation with an external source generated by the gauge field, while here the Higgs field obeys an NLS equation coupled with the gauge field. As previously explained, these two types of oscillons correspond to different scenarios for the underlying physics. We have performed simulations and confirmed the existence of robust oscillons described by Eqs. (2.22)-(2.23) in both Regions I and II for various values of q .

Additionally, our numerical findings support the existence of oscillons in the region where the perturbation scheme is not valid, i.e. for $1.88 < q < 2$. Using the same initial condition as above, we have integrated Eqs. (2.3)-(2.4) for $q = 1.95$ and the results are shown in the middle and bottom panels of Fig. 3. Since the system does not appear to support oscillons of the form of Eqs. (2.22)-(2.23), it is natural to expect a distortion of these type of solutions. Indeed, a large amount of radiation is emitted from the vicinity of the initially localized structure, as shown in the middle panel of Fig. 3. This panel depicts the short time evolution of A , and it is clearly seen that the distortion of the core starts very early. However, after sufficient time, a localized oscillating structure, different from the initial one, is formed and remains undistorted through the time of the evolution. The energy density of this oscillon is shown in the bottom panel of Fig. 3. The same qualitative result was observed for different values of q in this region (results not shown here), suggesting that oscillons do exist but they are not described by Eqs. (2.22)-(2.23). For completeness, the short time evolution of an oscillon in Region I is plotted in the top panel of Fig. 3, to highlight the fact that the radiation of the *true* oscillon solution (see Ref. [3]) has much

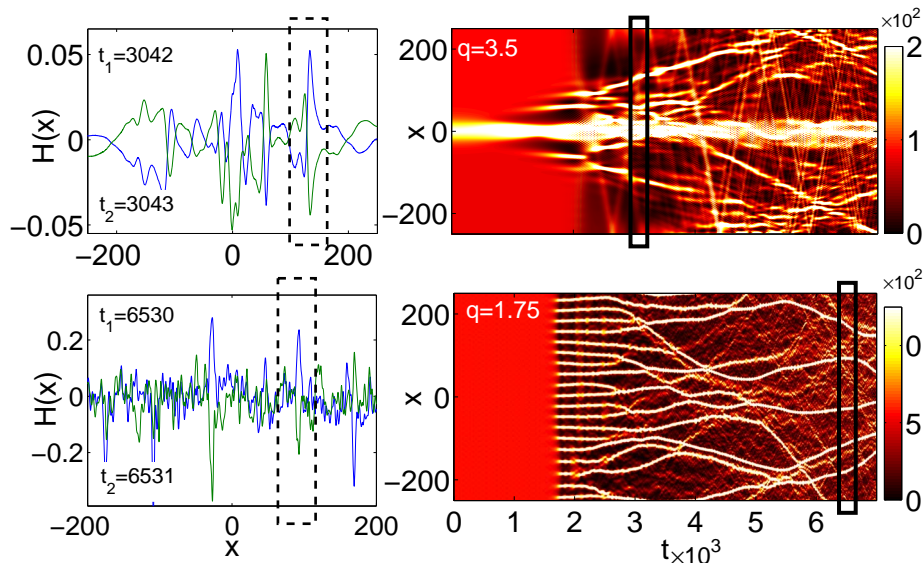


Figure 4: (Color online): Top left panel: profile snapshots of the field H at two different instants, $t_1 = 3042$ upper solid (blue) line and $t_2 = 3043$ lower solid (green). Dashed (black) box focuses on a single oscillon showing its oscillation in half period. Top right panel: Contour plot showing the evolution of the energy density $E(x, t)$ for a bd initial condition. The black box indicates the time of the snapshot. Bottom panels are the same as the top panels for plane wave initial conditions. In both contours the values of q are indicated in the upper left corner, and the time interval is $t = 7 \times 10^3$.

smaller amplitude than the oscillon.

Next, we perform numerical integration of the exact system of equations in the regions of q where solutions in the form of Eqs. (2.26)-(2.27) are expected to be subject to the MI mechanism. The evolution of the total energy for such a bd soliton is shown in the top right panel of Fig. 4 for $q = 3.5$. We observe that at $t \sim 2 \times 10^3$ the initially localized solution deforms and the instability settles in. Through the instability, localized structures occur on top of the initial solution (see e.g. the black box around $t = 3042$) having the form of oscillons. As an example, the profile of the Higgs field for $t = 3042$ and $t = 3043$ is shown in the top left panel of Fig. 4. The dashed box indicates an oscillon performing a half oscillation period. The above result is in agreement with our analytical findings regarding the instability of the oscillating kinks.

We conclude our numerical analysis by showing in the bottom panels of Fig. 4 the generation of oscillons at $q = 1.75$, that is in the db region. We have used initial conditions of the form: $A = H = C_0 [1 + \delta \cos(Kx)]$, where $C_0 = 0.05$ and $\delta = 10^{-2}$ are the plane wave and the perturbation amplitude respectively and $K = 0.025$ is a wavenumber inside the instability band given by Eq. (2.36). The initial, almost flat profile of the energy density deforms into a periodic pattern at $t \approx 2 \times 10^3$, due to the modulational-instability-induced exponential growth of the wavenumber K . At later times moving oscillons are formed, which are subject to collisions and eventually some survive and some annihilate. The time

interval indicated by the solid (black) box in the bottom right panel of Fig. 4 contains two time instants for which we show the Higgs field profile in the respective left panel. The dashed box focuses on a single oscillon at $x \approx 100$ performing a half oscillation period. Upper solid (blue) line corresponds to $t_1 = 6530$ and lower solid (green) line to $t_2 = 6531$. The oscillon performs oscillations with period $T_{osc} = 2\pi/q$ in agreement with the analytical predictions.

4 Conclusions and discussion

In conclusion, we have presented approximate analytical solutions of the (1+1)-dim Abelian-Higgs model, when the amplitudes of the gauge and the Higgs field are of the same order. Employing a multiple scale perturbation theory we reduced the original set of equations into a system of CNLS equations which admits different types of exact analytical solutions, depending on the parameter q (i.e. the ratio of two field masses).

Our analysis reveals that bright-bright solitons of the CNLS equations lead to robust long-lived oscillon solutions of the original system. These oscillons are characterized by symmetric oscillations around the “classical vacuum” (in contrast to the previous results of [19]), for both the gauge and the Higgs field, describing excitations which may occur when the gauge symmetry is strongly broken. Direct numerical simulations of the original system of equations of motion, confirm the robustness of the obtained solutions for times up to 5×10^4 oscillation periods. These oscillons are shown to exist in two different regions: $0.76 < q < 1.06$ (Region I) and $2.13 < q < 2.63$ (Region II). Note that one possible interpretation of our solutions is that oscillons with mass ratio less than unity (Region I) correspond to type-I superconductors, while oscillons of Region II, to type-II superconductors. This is compatible with the statements reported in Ref. [21], for the Abelian-Higgs in (3 + 1)-dim.

Using the derived CNLS system we have also shown that for any value of the parameter q , plane waves are subject to the modulation instability mechanism. Dark-bright (bright-dark) solitons and the corresponding oscillating kinks were found to be unstable, and their instability was shown to lead into oscillon-like patterns. Conclusively, it can be stated that in the (1 + 1)-dim Abelian-Higgs model, oscillons dominate the solution space of the involved fields.

The methodology used in the present work, may be applied in order to obtain novel localized structures in different settings, either with different potentials for the scalar field, or even in the presence of non-Abelian gauge fields [22]. A direct generalization would be to obtain an analytical form of oscillon solutions, in two and three dimensional settings.

The approximate analytical oscillon solutions presented here allows to study oscillon-oscillon interactions and characterize the stability of these structures upon collisions [8]. Since oscillons can be formed spontaneously (either from the modulation instability mechanism or due to other mechanisms such as parametric resonance), they are inevitably subject to mutual collisions influencing the long time field dynamics. Such studies are currently in progress.

References

- [1] R. F. Dashen, B. Hasslacher, and A. Neveu, *Phys. Rev. D* **11**, 3424 (1975).
- [2] I. L. Bogolyubskii, and V. G. Makhan'kov, [*JETP Lett.* **24**, 12 (1976)]; I. L. Bogolyubskii, and V. G. Makhan'kov, *JETP Lett.* **25**, 107 (1977).
- [3] H. Segur, and M. D. Kruskal, *Phys. Rev. Lett.* **58**, 747 (1987).
- [4] G. Fodor, P. Forgács, Z. Horváth, and M. Mezei, *Phys. Rev. D* **79**, 065002 (2009).
- [5] M. P. Hertzberg, *Phys. Rev. D* **82**, 045022 (2010).
- [6] D. K. Campbell, J. F. Schonfeld, and C. A. Wingate, *Physica, D* **9**, 1 (1983).
- [7] M. Gleiser, and A. Sornborger, *Phys. Rev. E* **62**, 1368 (2000).
- [8] M. Hindmarsh, and P. Salmi, *Phys. Rev. D* **74**, 105005 (2006).
- [9] M. Hindmarsh, and P. Salmi, *Phys. Rev. D* **77**, 105025 (2008).
- [10] M. Gleiser, *Phys. Rev. D* **49**, 2978 (1994); M. Gleiser, and R. M. Haas, *Phys. Rev. D* **54**, 1626 (1996).
- [11] E. J. Copeland, M. Gleiser, and H. -R. Müller, *Phys. Rev. D* **52**, 1920 (1995).
- [12] E. P. Honda, and M. W. Choptuik, *Phys. Rev. D* **65**, 084037 (2002).
- [13] G. Fodor, P. Forgács, P. Grandclément, and I. Rácz, *Phys. Rev. D* **74**, 124003 (2006).
- [14] M. Gleiser, and D. Sicilia, *Phys. Rev. Lett.* **101**, 011602 (2008); M. Gleiser, and D. Sicilia, *Phys. Rev. D* **80**, 125037 (2009).
- [15] M. Gleiser, *Phys. Lett. B* **600**, 126 (2004); P. M. Saffin, and A. Tranberg, *JHEP* **01**, 030 (2007).
- [16] G. Fodor, P. Forgács, Z. Horváth, and Á. Lukács, *Phys. Rev. D* **78**, 025003 (2008).
- [17] M. A. Amin, *Phys. Rev. D* **87**, 123505 (2013).
- [18] P. Arnold, and L. McLerran, *Phys. Rev. D* **37**, 1020 (1988).
- [19] V. Achilleos, F. K. Diakonou, D. J. Frantzeskakis, G. C. Katsimiga, X. N. Maintas, E. Manousakakis, C. E. Tsagkarakis, and A. Tsapalis, *Phys. Rev. D* **88**, 045015 (2013).
- [20] M. Gleiser, and J. Thorarinson, *Phys. Rev. D* **76**, 041701(R) (2007).
- [21] M. Gleiser, and J. Thorarinson, *Phys. Rev. D* **79**, 025016 (2009).
- [22] E. Farhi, N. Graham, V. Khemani, R. Markov, and R. Rosales, *Phys. Rev. D* **72**, 101701(R) (2005).
- [23] E. I. Sfakianakis, arXiv:hep-th/1210.7568.
- [24] N. Graham, *Phys. Rev. Lett.* **98**, 101801 (2007); N. Graham, *Phys. Rev. D* **76**, 085017 (2007).
- [25] M. Broadhead, and J. McDonald, *Phys. Rev. D* **72**, 043519 (2005); M. Gleiser, N. Graham, and N. Stamatopoulos, *Phys. Rev. D* **83**, 096010 (2011).
- [26] N. Graham, and N. Stamatopoulos, *Phys. Lett. B* **639**, 541 (2006); E. Farhi, N. Graham, A. H. Guth, N. Iqbal, R. R. Rosales, and N. Stamatopoulos, *Phys. Rev. D* **77**, 085019 (2008).
- [27] M. Gleiser, and N. Graham, arXiv:1401.6225.

- [28] M. A. Amin, R. Easther, and H. Finkel, *J. Cosmol.Astropart. Phys.* **12** (2010) 001; M. A. Amin, and D. Shirokoff, *Phys. Rev. D* **81**, 085045 (2010).
- [29] M. A. Amin, R. Easther, H. Finkel, R. Flauger, and M. P. Hertzberg, *Phys. Rev. Lett.* **108**, 241302 (2012).
- [30] S. Khlebnikov, L. Kofman, A. Linde, and I. Tkachev, *Phys. Rev. Lett.* **81**, 2012 (1998).
- [31] M. Gleiser, *Int. J. Mod. Phys. D* **16**, 219 (2007); A. Rajantie, and E. J. Copeland, *Phys. Rev. Lett.* **85**, 916 (2000).
- [32] M. Gleiser, N. Graham, and N. Stamatopoulos, *Phys. Rev. D* **82**, 043517 (2010).
- [33] A. Jeffrey, and T. Kawahara, *Asymptotic methods in nonlinear wave theory*, Pitman (1982).
- [34] X. N. Maintas, C. E. Tsagkarakis, F. K. Diakonou, and D. J. Frantzeskakis, *J. Mod. Phys.* **3**, 637 (2012), arXiv:hep-th/1306.6765; V. Achilleos, F. K. Diakonou, D. J. Frantzeskakis, G. C. Katsimiga, X. N. Maintas, C. E. Tsagkarakis, and A. Tsapalis, *Phys. Rev. D* **85**, 027702 (2012).
- [35] G. P. Veldes, J. Cuevas, P. G. Kevrekidis, and D. J. Frantzeskakis, *Phys. Rev. E* **88**, 013203 (2013).
- [36] The destabilization of plane waves under small-amplitude long-wavelength perturbations is known as modulational instability or Benjamin-Feir instability [T. B. Benjamin and J. E. Feir, *J. Fluid Mech.* **27**, 417 (1967)], and occurs in various contexts, including fluid mechanics [G. B. Whitham, *J. Fluid Mech.* **22**, 273 (1965)], dielectrics [L. A. Ostrovsky, *Sov. Phys. JETP* **24**, 797 (1967)], plasmas [A. Hasegawa, *Phys. Fluids* **15**, 870 (1972)], etc.
- [37] S. V. Manakov, and *Zh. Eksp. Teor. Fiz.* **65**, 505 (1973) [*Sov. Phys. JETP* **38**, 248 (1973)].